

Mapping of collision frequencies for stearic acid spin labels by saturation-recovery electron paramagnetic resonance

Jun-Jie Yin, Jim B. Feix, and James S. Hyde

National Biomedical ESR Center, Department of Radiology, Medical College of Wisconsin, Milwaukee, Wisconsin 53226 USA

ABSTRACT Short pulse saturation-recovery electron paramagnetic resonance methods have been used to measure interactions of ^{14}N : ^{15}N stearic acid spin label pairs in multilamellar liposomal dispersions composed of dimyristoylphosphatidylcholine (DMPC) and dielaidoylphosphatidylcholine (DEPC). Pairs consisting of various combinations of [^{14}N]-16-, [^{14}N]-12- or [^{14}N]-5-doxylstearate, and [^{15}N]-16-, [^{15}N]-12-, or [^{15}N]-5-doxylstearate were studied. SR experiments were performed at 27° and 37°C, and recovery signals were analyzed for initial conditions and multiexponential time constants by computer fitting using a damped least-squares approach. The time constants contain combinations of the electron spin lattice relaxation time, T_{1e} , for each member of the spin-label pair, and the Heisenberg exchange rate constant, K_x . Spin-lattice relaxation times for each of the ^{14}N and ^{15}N stearic acid spin labels were determined, and it is noted that T_{1e} for a given ^{15}N -SASL was always slightly greater than that of the corresponding ^{14}N -SASL. From K_x the bimolecular collision frequency was calculated, providing a detailed picture of molecular interactions. For both lipid systems the bimolecular collision rates were ordered as 12:5 < 16:5 < 5:5 < 16:12 < 12:12 < 16:16. For all spin-label pairs studied, interaction frequencies were greater in DMPC than in DEPC. For the 16:16, 12:12, and 16:12 pairs, K_x was ~30% greater in DMPC than in DEPC, a significantly greater difference than is observed by conventional EPR methods. Further confirmation of the existence of vertical fluctuation of nitroxide moieties that are at the 16- (or 12) position toward the polar surfaces was obtained, with the frequency of 16:5 (or 12:5) interactions ~40% of the 16:16 (or 12:12) interaction frequency. In both DMPC and DEPC, K_x for homogeneous pairs increases as the doxyl moiety is moved further down the alkyl chain (i.e., 5:5 < 12:12 < 16:16), suggesting that steric effects or the local rotational mobility of the nitroxide group influence the frequency at which spin exchange occurs.

INTRODUCTION

Many fundamental processes in membranes and cells depend on molecular motions of membrane components. In particular, translational diffusion is thought to be important in enzyme-acceptor interactions, embryological development, membrane phase separations, cell fusion, and membrane transport processes (1–5). Methods that measure the diffusion of membrane components also provide an important means to characterize the physical state of the membrane bilayer.

Previously we introduced electron-electron double resonance (ELDOR)¹ and saturation recovery (SR) electron paramagnetic resonance (EPR) methods for examining

the interaction of spin-labeled membrane components (6–12). These are “ T_1 -sensitive” methods, dependent on competition between electron spin-lattice relaxation and energy transfer caused by Heisenberg exchange, thus providing a direct measure of the bimolecular collision rate constant (K_x) between spin labels (for recent reviews see references 13 and 14). Conventional EPR methods for examining spin-spin interactions are “ T_2 -sensitive,” with the basis for measuring collision frequencies based on Heisenberg exchange-induced line broadening (15, 16). To ensure a significant contribution of the Heisenberg exchange frequency to the spectral linewidth, high concentrations (i.e., >2 mol %) of spin label are required. With ELDOR and SR, much lower spin-label concentrations (e.g., 0.1–0.5 mol % for lipid analogue spin labels in membranes) are needed, and complications due to contributions from mechanisms other than Heisenberg exchange are avoided.

In this work we utilize short pulse SR to study the interaction of stearic acid spin labels in model membranes. Analysis of the multiexponential return of the spin system to equilibrium after a short, saturating

Address correspondence to Dr. J. S. Hyde.

¹*Abbreviations used in this paper:* CSL, cholestane spin labels; CW ELDOR, continuous wave electron-electron double resonance; DEPC, dielaidoylphosphatidylcholine; DMPC, dimyristoylphosphatidylcholine; EPR, electron paramagnetic resonance; K_x , bimolecular collision-rate constant; N_I and N_{II} , concentrations of ^{14}N and ^{15}N spin labels, respectively, in mole %; n -SASL, n -doxyl stearic acid spin label; SR, saturation recovery; T_{1e} , spin-lattice relaxation time; W_e , electron spin-lattice relaxation rate; W_n , nuclear spin-lattice relaxation rate; W_x , Heisenberg spin exchange frequency.

microwave pulse gives the electron spin-lattice relaxation rates (W_{12} , W_{34}) for the ^{14}N and ^{15}N probes, respectively, as well as K_x (9). Additionally, we have shown that under certain experimental conditions, no matter how spin-label spectra are overlapped or where the EPR resonance condition is set in the spectrum, the time constants obtained from the superimposed exponentials are always the same; only the prefactors are changed (10). This overcomes the spectral resolution problem, which often limits the applicability of field-swept ELDOR.

As in our previous ELDOR and SR studies we employ ^{14}N : ^{15}N spin-label pairs, in which nitroxide spin labels of each isotope are introduced independently into the sample. The use of two spin-label populations allows the study of interactions between nitroxides attached to different types of macromolecules or, in the case of the stearic acid spin labels, at different positions along the alkyl chain (7, 11). ELDOR studies have given collision frequencies between ^{14}N -16 doxyl-stearate and ^{15}N -16 doxylstearate (i.e., the 16:16 pair) intercalated into model membrane bilayers that are consistent with lateral diffusion rates for lipids in membranes (7, 8, 11). We have also observed a strong interaction of the 16:5 pair, which in pure phosphatidylcholine bilayers approaches 40% of the lateral diffusion limit (given by the 16:16 pair). The vertical fluctuations of the 16-doxylstearate probe that gives rise to the 16:5 interaction are sensitive to temperature, pH, and membrane composition (7, 11, 12). However, studies of the interaction between other stearic acid spin-label pairs have been limited by spectral resolution considerations.

Here we extend our studies to provide a more complete mapping of the interactions between doxyl stearic acid spin labels. We also compare collision rates in bilayers of dimyristoylphosphatidylcholine (DMPC), with 14 carbon saturated alkyl chains, and dielaidoylphosphatidylcholine (DEPC), with 18 carbon alkyl chains each containing a *trans* double bond.

MATERIALS AND METHODS

The *n*-doxyl steric acid spin labels (*n*-SASLs) containing ^{15}N substituted nitroxide moieties at the 5, 12, and 16 positions ($^{15}\text{NC5}$, $^{15}\text{NC12}$, and $^{15}\text{NC16}$, respectively) were synthesized according to the method of Joseph and Lai (17). The corresponding ^{14}N *n*-SASLs ($^{14}\text{NC5}$, $^{14}\text{NC12}$, and $^{14}\text{NC16}$) were obtained from Aldrich Chemical Co. (Milwaukee, WI).

DMPC and DEPC were from Sigma Chemical Co. (St. Louis, MO.).

Stock solutions of the spin labels and lipids were prepared in chloroform and stored at -20°C . Multilamellar liposomes were prepared by directly hydrating the dried lipids and spin labels with an appropriate amount of buffer as described previously (7). The buffer was 0.1 M borate, pH 9.5 to insure that all stearic acid carboxyl groups in the phosphatidylcholine membranes were ionized (reference 7 and references therein). All samples were run in capillaries made of the methylpentene polymer TPX (0.6 mm id). A flow of temperature-

regulated nitrogen gas over the capillary was used to remove oxygen (18).

Conventional EPR spectra were obtained on a spectrometer (Century Series; Varian Associates, Inc., Palo Alto, CA) in normal configuration. Spectra were obtained with 5 mW incident microwave power and 100 kHz field modulation of 0.5 G. The order parameter, S , was calculated as previously described (19). Anisotropic rotational correlation times were calculated from the average of the linear and quadratic terms (20, 21).

The continuous wave (CW) ELDOR technique was used to estimate the ratio of the nuclear spin-lattice relaxation rate, W_n , to the electron spin-lattice relaxation rate, W_e (6). The measurements were performed as described previously using a loop-gap resonator (22). ELDOR reductions were measured on the center line of ^{14}N when the low field line was pumped. The separation was 44 MHz between the two microwave frequencies.

The CW ELDOR reduction factor was determined at a series of nine pumping intensities and R^{-1} plotted against the inverse pumping power, P^{-1} (23). Extrapolation to infinite pumping power gives the intercept R_∞^{-1} , which is a function of the relaxation process occurring in the spin system. With low spin-label concentrations, the relaxation process is dominated by nuclear spin-lattice relaxation, and from reference 24,

$$R_\infty(\text{END}) = \frac{b + b^2}{1 + 3b + b^2},$$

$$b = W_n/W_e. \quad (1)$$

The saturation-recovery spectrometer is based on the design of Huisjen and Hyde (25). A multichannel signal acquisition system greatly improves the signal-to-noise ratio over what could be achieved with the single channel boxcar. A field-effect transistor microwave amplifier has been introduced. The time response limit is 0.1 μs . A high-order low-pass filter at the input to the analogue/digital converter cuts off at 25 MHz, which results in minimal distortion of the transient signal. Typically, 2×10^4 decays per second were acquired with 512 data points per decay. Total accumulation time was 5 min. Aperture intervals were 40 ns at 37°C and 60 ns at 27°C .

Short pulse saturation-recovery experiments were performed as in our previous studies (8, 10). As a control, every experiment was run with different pump durations because the time constants of the multiexponentials are independent of the width of the pump pulse (8).

For the general case of interacting ^{14}N and ^{15}N spin systems, the saturation-recovery experiment is expected to give five superimposed exponentials (8). However, under the condition that $W_n \gg W_e$ the nuclear spin states within each isotopic system are strongly coupled, and a simplified relaxation model can be used in which only two superimposed exponentials are observed (10). The ratio of W_n to W_e , b (Eq. 1), can be determined by CW ELDOR (6) to check the validity of this assumption.

From reference 10 the saturation-recovery signal is:

$$i_{\text{sr}} = I_1 e^{-(A-B)t} + I_2 e^{-(A+B)t}, \quad (2)$$

where

$$A = W_{12} + W_{34} + (1/2)K_x(N_I + N_{II}), \quad \text{and} \quad (3)$$

$$B = [(W_{12} - W_{34})^2 - K_x(N_I - N_{II})(W_{12} - W_{34}) + (1/4)K_x^2(N_I + N_{II})^2]^{1/2}. \quad (4)$$

W_{12} and W_{34} , the spin-lattice relaxation rates [$= 1/(2T_{1e})$] of the ^{14}N and ^{15}N spin labels, were measured independently by SR in membranes

containing either the ^{14}N or ^{15}N species alone (Table 1). N_i and N_{ii} are the ^{14}N and ^{15}N spin-label concentrations, respectively, expressed as mole % of the total phospholipid. Computer modeling of the experimental SR curve for a given ^{14}N : ^{15}N pair gives a double exponential with time constants $(A - B)$ and $(A + B)$, as in Eq. 2. Addition of these time constants gives A and, knowing W_{12} , W_{34} , N_i , and N_{ii} , K_x is calculated from Eq. 3. Raw data for the various spin-label pairs are given in Table 2.

The theoretical models were compared with experimental saturation-recovery curves using the damped least-squares method, which has proven successful for fitting overlapping exponential decay curves (26) and EPR spectra (27). This method utilizes the Gauss-Newton minimization procedure to which a scalar factor is included, thus helping to "damp" the process toward the minimum and assuring convergence. In some cases experimental spectra were smoothed by means of autocorrelation. Results with smoothed and unsmoothed spectra were in good agreement. The curve-fitting program was run on an IBM PC/AT computer.

RESULTS

Conventional EPR spectra for the various combinations of ^{14}N and ^{15}N -SASLs in fluid-phase DMPC are shown in Fig. 1. For samples in which the motion of the ^{14}N probe is relatively fast (e.g., Fig. 1, A–C), the ^{14}N and ^{15}N resonances in the low-field region are reasonably well resolved, and the interaction frequencies for these pairs have been examined previously by CW ELDOR methods (7, 11). For the remaining pairs (Fig. 1, D–F), there is considerable spectral overlap throughout the spectra and only the short pulse SR method will give reliable bimolecular collision rates.

Spin-lattice relaxation times for the individual species of SASLs are given in Table 1. T_{1e} values become larger as effective rotational correlation times increase ($\text{C5} > \text{C12} > \text{C16}$ and $27^\circ\text{C} > 37^\circ\text{C}$ values), as expected from either spin-rotational (28) or electron-nuclear dipolar (29, 30) mechanisms. We also note that the T_{1e} for a given ^{15}N SASL is always slightly greater than that of the corresponding ^{14}N SASL. The basis for this is currently under investigation.

The very large ELDOR effects that arise due to nuclear relaxation are shown in Fig. 2 for $^{14}\text{NC16}$ (0.1 mol %) and $^{14}\text{NC12}$ (0.1 mol %) in DEPC at 37°C . As the motion becomes slower, e.g., 12-SASL compared with 16-SASL, the ELDOR effect becomes larger as a result of both increasing W_n and decreasing W_e . Table 3 shows the ELDOR reduction factor (R_∞) and the calculated ratio of W_n to W_e for $^{14}\text{NC12}$ and $^{14}\text{NC16}$ in DMPC and DEPC. W_n/W_e should be even greater for 5-SASL. These experiments clearly show that under our conditions nuclear spin relaxation is much faster than electron spin-lattice relaxation. A simplified relaxation model is appropriate and double exponential recoveries are expected.

A representative saturation-recovery signal, along with a simulated fit, is shown in Fig. 3 for the $^{14}\text{NC16}$: $^{15}\text{NC16}$ spin-label pair in DMPC at 27°C . The early points ($\sim 2 \mu\text{s}$) of the SR signals were discarded and the remaining part of the curve was fit to a double exponential. The Heisenberg spin exchange-rate constant, K_x , was calculated from the two recovery time constants and the known spin-lattice relaxation rates (Table 1) using Eqs. 1–3.

The bimolecular collision frequencies between 16-SASL of one isotope and the various positional isomers of the other isotopic species are shown in Fig. 4 A. In both DMPC and DEPC, at both 27° and 37°C , the interaction frequency was directly dependent on the separation of the nitroxide moieties along the alkyl chain, decreasing with increasing separation of the doxyl groups. Collision frequencies are always greater in DMPC than in DEPC, and increase with increasing temperature. Similar trends were observed with pairs involving 12-SASL (Fig. 4 B).

Bimolecular collision frequencies for pairs involving 5-SASL are shown in Fig. 4 C. K_x was greatest for the 5:5 pair. However, K_x for 16:5 was greater than that for 12:5 indicating that 16-SASL spends a greater proportion of time near the membrane surface than does 12-SASL.

Collision frequencies for the homogeneous pairs are shown in Fig. 5. Exchange rates increased progressively as

TABLE 1 Electron spin-lattice relaxation times (T_{1e}) for ^{14}N , ^{15}N SASL (μs)

Temp.	$^{14}\text{NC16}$	$^{14}\text{NC12}$	$^{14}\text{NC5}$	$^{15}\text{NC16}$	$^{15}\text{NC12}$	$^{15}\text{NC5}$
$^\circ\text{C}$						
DMPC						
27	2.52	4.41	5.33	2.80	4.80	5.41
37	2.19	3.62	4.21	2.19	3.92	4.28
DEPC						
27	2.67	4.60	5.46	3.08	5.09	5.80
37	2.20	3.91	4.40	2.49	4.26	4.70

Samples contained a single species of either ^{14}N or ^{15}N SASL present in the liposomes at 0.1 mol %. The buffer was 0.1 M borate. Saturation-recovery experiments were performed using a saturating pulse ($5 \mu\text{s}$) comparable with or longer than T_{1e} , after which single exponential signals were obtained. Time constants were obtained from computer simulation as described in the text. Mean standard deviations are $\pm 0.08 \mu\text{s}$.

TABLE 2 Experimental decay and collision rate constants vs. spin label pairs at 27 (37)°C

Spin label pair	16:16	16:12	16:5	12:12	12:5	5:5
DMPC						
$(A - B)^{-1} \mu s$	2.51 ± 0.07 (2.10 ± 0.06)	2.85 ± 0.10 (2.53 ± 0.08)	3.17 ± 0.10 (2.67 ± 0.09)	4.35 ± 0.10 (3.54 ± 0.06)	4.55 ± 0.20 (3.65 ± 0.12)	5.29 ± 0.23 (4.22 ± 0.12)
$(A + B)^{-1} \mu s$	1.07 ± 0.06 (0.93 ± 0.04)	1.44 ± 0.08 (1.21 ± 0.05)	2.04 ± 0.08 (1.74 ± 0.08)	1.55 ± 0.08 (1.20 ± 0.05)	2.56 ± 0.10 (2.08 ± 0.08)	2.12 ± 0.09 (1.62 ± 0.08)
$K_x (MHz/mol \%)$	0.77 (0.85)	0.58 (0.67)	0.29 (0.34)	0.59 (0.78)	0.26 (0.30)	0.38 (0.51)
DEPC						
$(A - B)^{-1} \mu s$	2.79 ± 0.08 (2.34 ± 0.07)	3.18 ± 0.10 (2.72 ± 0.07)	3.85 ± 0.12 (2.95 ± 0.10)	4.77 ± 0.07 (4.01 ± 0.06)	5.10 ± 0.18 (4.26 ± 0.11)	5.50 ± 0.20 (4.45 ± 0.15)
$(A + B)^{-1} \mu s$	1.31 ± 0.08 (1.10 ± 0.06)	1.70 ± 0.04 (1.42 ± 0.04)	2.14 ± 0.08 (1.79 ± 0.08)	1.78 ± 0.05 (1.51 ± 0.05)	2.75 ± 0.10 (2.30 ± 0.10)	2.37 ± 0.10 (1.76 ± 0.08)
$K_x (MHz/mol \%)$	0.56 (0.64)	0.42 (0.51)	0.24 (0.31)	0.47 (0.56)	0.23 (0.27)	0.33 (0.47)

$(A - B)^{-1}$, $(A + B)^{-1}$ values are from computer simulations of samples containing ^{14}N (0.5 mol %) and ^{15}N (0.25 mol %) spin labels at 27°C (i.e., $N_I = 0.5$, $N_{II} = 0.25$). Values in parentheses are for 37°C. K_x was calculated from Eq. 3 as described in the text.

the nitroxide moieties were moved further down the alkyl chain.

DISCUSSION

In this study we have utilized the short pulse saturation-recovery method to examine the interactions between stearic acid spin labels in model membrane bilayers. Such studies provide insight into the motional dynamics of lipid-analogue spin labels in the bilayer and the manner in which motion is modulated by membrane composition. In the present work we find that, for both DMPC and DEPC

at 27° and 37°C, bimolecular collision frequencies for the spin-label pairs are ordered as $12:5 < 16:5 < 5:5 < 16:12 < 12:12 < 16:16$. These studies further confirm the occurrence of vertical fluctuations of nitroxide moieties at



FIGURE 1 ESR spectra of six combinations of ^{14}N and ^{15}N -nSASL. Samples contain 0.5 mol % ^{14}N spin label and 0.25 mol % ^{15}N spin label in DMPC, equilibrated with 0.1 M sodium borate, pH 9.5 at 37°C. (A) 16:16, (B) 16:12, (C) 16:5, (D) 12:12, (E) 12:5, (F) 5:5.

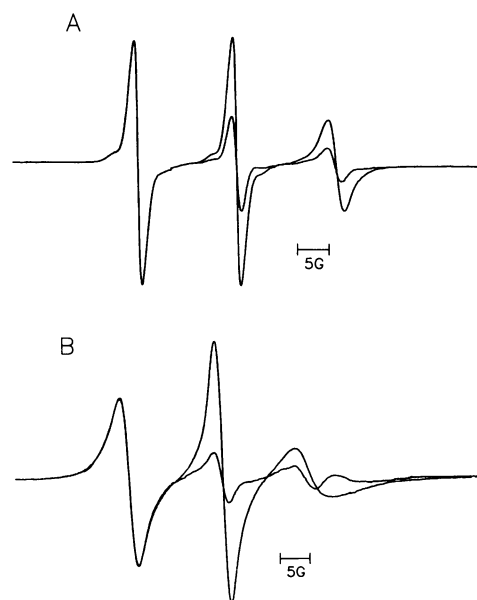


FIGURE 2 The CW ELDOR effect for (A) $^{14}NC16$ (0.1 mol %) and (B) $^{14}NC12$ (0.1 mol %) steric acid spin labels in DEPC at 37°C, pH 9.5. Shown are superimposed spectra taken with the pump field off and at 100 mW. ELDOR reductions were measured on the center line when the low field line was pumped. The separation was 44 MHz between the two microwave frequencies.

TABLE 3 CW ELDOR results

Temp.	Spin label	Host lipid	R_∞	W_n/W_e
°C				
27	$^{14}\text{NC16}$	DMPC	0.88 ± 0.05	13.8 ± 5
27	$^{14}\text{NC16}$	DEPC	0.83 ± 0.02	9.3 ± 3
37	$^{14}\text{NC16}$	DMPC	0.65 ± 0.03	3.4 ± 0.4
37	$^{14}\text{NC16}$	DEPC	0.70 ± 0.05	4.5 ± 0.8
37	$^{14}\text{NC12}$	DMPC	0.96 ± 0.01	47.5 ± 8
37	$^{14}\text{NC12}$	DEPC	0.95 ± 0.01	34.0 ± 10

R_∞ values are the inverse of R_2^{-1} , determined as described in text. W_n/W_e was calculated according to Eq. 1. Samples contained 0.1 mol % spin label in the designated lipid. R_∞ and W_n/W_e values are mean \pm SD from three experiments each.

the 16- (or 12) position toward the bilayer surface (7, 11, 31, 32). Interaction of the 16:5 pair occurs at a frequency slightly $>12:5$ interaction, indicating that the nitroxide moiety of 16-SASL has a greater propensity for approaching the membrane surface than does 12-SASL.

We have previously used the ratio $K_x(16:5)/K_x(16:16)$, which normalizes the 16:5 collision rate to the limits imposed by lateral diffusion, for comparison of vertical fluctuations in different host lipids (11). In the present work $K_x(16:5)/K_x(16:16)$ was 0.40 in DMPC at 37°C, in excellent agreement with our earlier ELDOR study (11). Surprisingly, this ratio was 0.48 in DEPC at 37°C, indicating an even greater occurrence of vertical fluctuations. This is in sharp contrast to the significant decrease in vertical fluctuations observed in POPC [1-palmitoyl-2-oleoylphosphatidylcholine], which has a single *cis* double bond in the *sn*-2 alkyl chain (11). Whether these differences are due to the *trans* nature of the double bonds in DEPC, or to the fact that all alkyl chains in DEPC are similarly unsaturated (as opposed to the mixture of saturated and unsaturated alkyl chains in POPC) de-

serves further investigation. Very similar values are obtained for the ratio $K_x(12:5)/K_x(12:12)$, indicating that the trends observed are not peculiar to the particular spin-label pairs chosen for comparison.

Collision frequencies were greater in DMPC than in DEPC for all spin-label pairs examined (Fig. 4). This is consistent with a lower degree of structural order (i.e., less restriction of spin-label mobility) in DMPC, also indicated by conventional EPR order parameters (Table 4). An increase in the molecular volume of DEPC relative to DMPC (33) may also contribute to the decreased bimolecular collision rates observed in DEPC. The greater interaction in DMPC was particularly evident for pairs involving 12- and 16-SASL, with the ratio of exchange frequencies in the two membrane systems, i.e., $K_x(\text{DMPC})/K_x(\text{DEPC})$, for 16:16, 16:12, and 12:12 pairs being 1.38, 1.38; 1.25 at 27°C and 1.33, 1.31, 1.39 at 37°C, respectively. These differences in exchange frequency of ~ 30 –40% between the two systems are significantly greater than differences in order parameter observed by conventional EPR methods (Table 4).

In both DMPC and DEPC, collision frequencies for homogeneous pairs increase in the order $5:5 < 12:12 < 16:16$. These results suggest that steric effects or local motional modes, i.e., rotational mobility, may influence the frequency at which exchange events occur. The doxyl group of 16-SASL explores a much larger volume than that of 5-SASL (with 12-SASL intermediate) on the time scale of the experiment, providing greater opportunity for collisions.

It is also conceivable that interaction between probes in opposite leaflets of the bilayer contribute to the collision frequency for the 16:16 pair. This would effectively double the concentration of spin label available for interaction for 16:16 relative to the other spin-label pairs. $K_x(16:16)/K_x(5:5)$ in DMPC is 1.67 at 37°C and 2.03 at 27°C (where vertical fluctuations are diminished and 16-SASL is expected to spend a greater proportion of time near the center of the bilayer). However, $K_x(16:16)/K_x(5:5)$ in DEPC is only 1.36 at 37°C (1.50 at 27°C), despite the fact that the difference in bilayer thickness

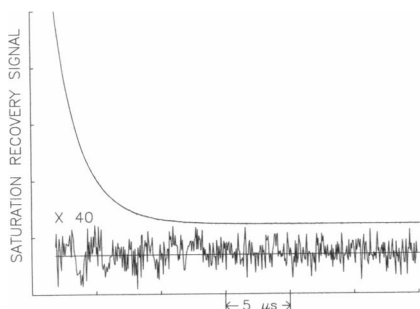


FIGURE 3 Saturation-recovery signal and curve fitting for $^{14}\text{NC16}$: $^{15}\text{NC16}$ (0.5:0.25 mol %) in DMPC at 27°C, pH 9.5. The recovery curve contains 512 data points with a resolution of 60 ns per point. Simulations and experimental saturation-recovery signals are superimposed. The difference, multiplied by a factor of 40, is shown as the “residual” beneath the recovery curve. Each recovery signal was obtained in 5 min at 20,000 accumulations per second. The time constants for this fit are 2.48 and 1.06 μs .

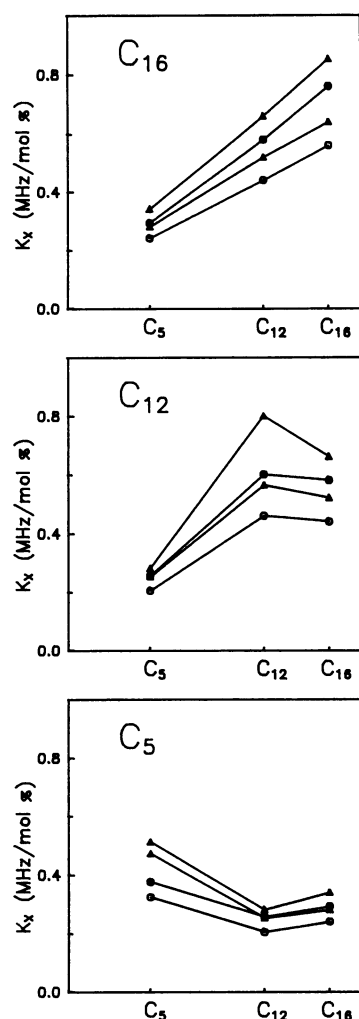


FIGURE 4 Bimolecular collision rate constants for a nitroxide moiety at the C₁₆, C₁₂, or C₅ position of the stearic acid alkyl chain with other SASLs in (●) DMPC, 27°C; (○) DEPC, 27°C; (▲) DMPC, 37°C; and (△) DEPC, 37°C.

between DMPC and DEPC is only ~ 3 Å (33, 34). This suggests that the contribution of collisions between probes in opposite leaflets may be small. A previous ELDOR study indicated that there was little difference in the 16:16 interaction frequency in DMPC, DPPC, and distearoylphosphatidylcholine when compared at a constant reduced temperature (11), also suggesting that there is little interaction between probes in opposite leaflets. Additional experiments with lipids having more extreme differences in bilayer thickness may further clarify this matter.

The effects of orbital orientation on Heisenberg exchange are also unknown. Rapid motional averaging of the $2p\pi$ orbital (containing the majority of the unpaired

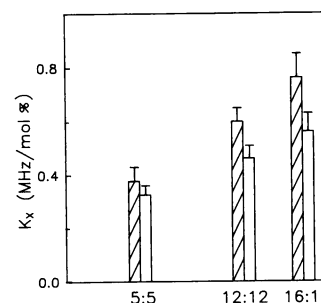


FIGURE 5 Bimolecular collision rate constants between ^{14}N and ^{15}N SASL for homogeneous pairs in DMPC (open bars) and DEPC (hatched bars) at 27°C. Similar trends were observed at 37°C.

spin density) for 12- and 16-SASL relative to the more highly oriented 5-SASL may also contribute to increased exchange efficiency per encounter. These factors, rather than changes in the rate of lateral diffusion, may also be the basis for relatively large differences in K_x for the 16:16 and 12:12 pairs in DMPC and DEPC noted above.

The collision frequencies for 5:5 in DMPC and DEPC are similar to those previously measured for interaction between cholestane spin labels (CSL) in DMPC (10). This suggests that collision frequencies measured with these labels (CSL and 5-SASL), which experience little or no vertical displacement due to trans-gauche interconversion of carbon-carbon bonds between the carboxyl head group and nitroxide moiety (19, 35, 36), may provide the best basis for calculation of lateral diffusion constants. These results also suggest that lateral diffusion of the stearic acid and cholesterol molecules in these systems are very similar.

In conclusion, by use of the short pulse saturation-recovery method to overcome problems due to spectral overlap, we have extended our mapping of the interactions between ^{14}N : ^{15}N spin-label pairs in model membrane bilayers. Collision frequencies between ^{14}N and ^{15}N stearic acid spin labels in DMPC are greater than in DEPC for all spin-label pairs studied. This is consistent with increased order in DEPC as determined by conventional EPR methods. However, differences in the two systems were much greater using the ^{14}N : ^{15}N approach developed here.

TABLE 4 Order parameters for SASLs in DMPC, DEPC

	27°C		37°C	
	DMPC	DEPC	DMPC	DEPC
$^{14}\text{NC5}$	0.626	0.637	0.586	0.596
$^{14}\text{NC12}$	0.205	0.213	0.167	0.184
$^{14}\text{NC16}$	0.100	0.103	0.076	0.088

We thank Dr. J. Joseph for the synthesis of the [^{15}N] fatty acid spin labels.

This work was supported by grants GM27665, GM22923, and RR01008 from the National Institutes of Health.

Received for publication 11 December 1989 and in final form 19 April 1990.

REFERENCES

1. Delaat, S. W., P. T. van der Saag, E. L. Elson, and J. Schlessinger. 1979. Lateral diffusion of membrane lipids and proteins is increased specifically in neurites of differentiating neuroblastoma cells. *Biochim. Biophys. Acta*. 558:247–250.
2. Stittmatt, W. J., and M. J. Rogger. 1975. Apparent dependence of interaction between cytochrome b_5 and cytochrome b_5 reductase upon translational diffusion in dimyristoyl lecithin liposomes. *Proc. Natl. Acad. Sci. USA*. 72:2658–2661.
3. Johnson, M., and M. Edidin. 1978. Lateral diffusion in plasma membrane of mouse egg is restricted after fertilization. *Nature (Lond.)*. 272:448–450.
4. Henis, Y. I., G. Rimon, and S. Felder. 1982. Lateral mobility of phospholipids in turkey erythrocytes. Implications for adenylate cyclase activation. *J. Biol. Chem.* 257:1407–1411.
5. Edidin, M. 1987. Rotational and lateral diffusion of membrane proteins and lipids: phenomena and function. *Curr. Top. Membr. Transp.* 29:91–127.
6. Popp, C. A., and J. S. Hyde. 1982. Electron-electron double resonance and saturation recovery studies of nitroxide electron and nuclear spin-lattice relaxation times and Heisenberg exchange rates: lateral diffusion in dimyristoyl phosphatidylcholine. *Proc. Natl. Acad. Sci. USA*. 79:2559–2563.
7. Feix, J. B., C. A. Popp, S. D. Venkataramu, A. H. Beth, J. H. Park, and J. S. Hyde. 1984. An electron-electron double resonance study on interaction between [^{14}N] and [^{15}N] steric acid and vertical fluctuation in dimyristoylphosphatidylcholine. *Biochemistry*. 23:2293–2299.
8. Yin, J.-J., M. Pasenkiewicz-Gierula, and J. S. Hyde. 1987. Lateral diffusion of lipids in membrane by pulse saturation recovery electron spin resonance. *Proc. Natl. Acad. Sci. USA*. 84:964–968.
9. Yin, J.-J., and J. S. Hyde. 1987. Application of rate equations to ELDOR and saturation recovery experiments on ^{14}N : ^{15}N spin label pairs. *J. Magn. Reson.* 74:82–93.
10. Yin, J.-J., J. B. Feix, and J. S. Hyde. 1988. Solution of the nitroxide spin-label spectral overlap problem using pulse electron spin resonance. *Biophys. J.* 53:1031–1038.
11. Feix, J. B., J.-J. Yin, and J. S. Hyde. 1987. Interactions of ^{14}N : ^{15}N stearic acid spin-label pairs: effects of host lipid alkyl chain length and unsaturation. *Biochemistry*. 26:3850–3855.
12. Yin, J.-J., J. B. Feix, and J. S. Hyde. 1987. The effects of cholesterol on lateral diffusion and vertical fluctuations in lipid bilayers. *Biophys. J.* 52:1031–1038.
13. Hyde, J. S., and W. K. Subczynski. 1989. Spin-label oximetry. In *Biological Magnetic Resonance*. L. J. Berliner and J. Reuben, editors. Plenum Publishing Corp., New York. 8:399–426.
14. Hyde, J. S., and J. B. Feix. 1989. Electron-electron double resonance. In *Biological Magnetic Resonance*. L. J. Berliner and J. Reuben, editors. Plenum Publishing Corp., New York. 8:305–339.
15. Devaux, P., and H. M. McConnell. 1972. Lateral diffusion in spin labeled phosphatidylcholine multilayers. *J. Am. Chem. Soc.* 94:4475–4481.
16. Sackmann, E., and H. Träuble. 1972. Studies of the crystalline-liquid crystalline phase transition of lipid model membranes. II. Analysis of electron spin resonance spectra of steroid labels incorporated into lipid membranes. *J. Am. Chem. Soc.* 94:4492.
17. Joseph, J., and C.-S. Lai. 1987. An improved synthesis of [^{15}N] 16-doxyl stearic acid. *J. Labelled Compd. & Radiopharm.* 24:1159–1165.
18. Popp, C. A., and J. S. Hyde. 1981. Effect of oxygen on ESR spectra of nitroxide spin-label probes of model membranes. *J. Magn. Reson.* 43:249–258.
19. Hubbell, W. L., and H. M. McConnell. 1971. Molecular motions in spin-labeled phospholipids and membranes. *J. Am. Chem. Soc.* 93:314–326.
20. Kivelson, D. 1960. Theory of ESR linewidths of free radicals. *J. Chem. Phys.* 33:1094–1106.
21. Freed, J. H., and G. K. Fraenkel. 1963. Theory of linewidths in electron spin resonance spectra. *J. Chem. Phys.* 39:326–348.
22. Hyde, J. S., J.-J. Yin, W. Froncisz, and J. B. Feix. 1985. Electron-electron double resonance (ELDOR) with a loop-gap resonator. *J. Magn. Reson.* 63:142–150.
23. Eastman, M. P., G. V. Bruno, and J. H. Freed. 1970. ESR studies of Heisenberg spin exchange. III. An ELDOR study. *J. Chem. Phys.* 52:321–327.
24. Hyde, J. S., J. C. W. Chien, and J. H. Freed. 1968. Electron-electron double resonance of free radical in solution. *J. Chem. Phys.* 48:4211–4226.
25. Huisjen, M., and J. S. Hyde. 1974. A pulse EPR spectrometer. *Rev. Sci. Instrum.* 45:669–675.
26. Laiken, S. L., and M. P. Printz. 1970. Kinetic class analysis of hydrogen exchange data. *Biochemistry*. 9:1547–1553.
27. Pasenkiewicz-Gierula, M., W. A. Antholine, W. K. Subczynski, O. Baffa, J. S. Hyde, and D. H. Petering. 1987. Assessment of the ESR spectra of CuKTSM₂. *Inorg. Chem.* 26:3945–3949.
28. Atkins, P. W., and D. Kivelson. 1966. ESR linewidth in solution. II. Analysis of spin-rotational relaxation data. *J. Chem. Phys.* 44:169–174.
29. Bloembergen, N., E. M. Purcell, and R. V. Pound. 1943. Relaxation effects in nuclear magnetic resonance absorption. *Phys. Rev.* 73:679–712.
30. McConnell, H. M. 1956. Effect of anisotropic hyperfine interactions on paramagnetic relaxation in liquids. *J. Chem. Phys.* 25:709–711.
31. Merkle, H., W. K. Subczynski, and A. Kusumi. 1987. Dynamic fluorescence quenching studies on lipid mobilities in phosphatidylcholine-cholesterol membranes. *Biochim. Biophys. Acta*. 897:238–248.
32. Wardlaw, J. R., W. H. Sawyer, and K. P. Ghiggino. 1987. Vertical fluctuations of phospholipid acyl chains in bilayers. *FEBS (Fed. Eur. Biochem. Soc.) Lett.* 223:20–24.
33. Cornell, B. C., and F. Separovic. 1983. Membrane thickness and acyl chain length. *Biochim. Biophys. Acta*. 733:189–193.

-
34. Caffrey, M., and G. W. Feigenson. 1981. Fluorescence quenching in model membranes. 3. Relationship between calcium adenosine-triphosphatase enzyme activity and the affinity of the protein for phosphatidylcholines with different acyl chain characteristics. *Biochemistry*. 20:1949-1961.
35. Seelig, A., and J. Seelig. 1974. The dynamic structure of fatty acyl chains in a phospholipid bilayer measured by deuterium magnetic resonance. *Biochemistry*. 13:4839-4845.
36. Schindler, H., and J. Seelig. 1975. Deuterium order parameter in relation to thermodynamic properties of a phospholipid bilayer. A statistical mechanical interpretation. *Biochemistry*. 14:2283-2287.